OncoTargets and Therapy

Dovepress
open access to scientific and medical research

Open Access Full Text Article

ORIGINAL RESEARCH

RETRACTED ARTICLE: microRNA-130a is an oncomir suppressing the expression of *CRMP4* in gastric cancer

This article was published in the following Dove Press journal:
OncoTargets and Therapy
3 August 2017
Number of times this article has been viewed

Yiran Zhou[1,2,*]
Ruhong Li[2,*]
Haidong Yu[2]
Ruotian Wang[2]
Zhiqiang Shen[1]

[1]Department of Pharmacy, Kunming Medical University, [2]Yan'an Hospital Affiliated to Kunming Medical University, Kunming, People's Republic of China

*These authors contributed equally to this work

Abstract: Gastric cancer is one of the most common causes of death worldwide, although its incidence has steadily declined in recent years. There is strong evidence that aberrantly expressed microRNAs (miRNAs) are involved in gastric cancer tumorigenesis. Furthermore, *CRMP4* is closely associated with the occurrence and development of gastric cancer, and our predictions suggest that miR-130a, which can promote gastric cancer tumorigenesis, is a potential *CRMP4* regulator. In this study, we investigated the expression of *CRMP4* and miR-130a in human gastric cancer cell lines by quantitative reverse transcription polymerase chain reaction (qRT-PCR) and Western blot (WB) examination and direct interactions between miR-130a and *CRMP4* by dual-luciferase reporter assay. We also evaluated the biological roles of miR-130a and *CRMP4* in gastric cancer cells by flow cytometry, MTT assay, soft agar colony formation assay, and Transwell tests and confirmed *CRMP4* function in vivo, using a tumor xenograft model. Our results demonstrated that *CRMP4* expression was significantly decreased at both the gene and protein levels, while miR-130a expression was notably increased, in five human gastric cancer cell lines compared with human gastric epithelial cells. Dual-luciferase reporter assays indicated that *CRMP4* was the direct target of miR-130a. Moreover, an inverse regulatory relationship between miR-130a and *CRMP4* was verified by qRT-PCR and WB, and overexpression of miR-130a in BGC823 cells enhanced apoptosis and cell proliferation, arrested the cell cycle in G0/G1, and facilitated cell colony formation, invasion, migration, and adhesion, while upregulation of *CRMP4* had opposite effects. Finally, the growth and weight of transplanted tumors derived from BGC823 cells in which *CRMP4* was knocked down were remarkably reduced. These data indicate that miR-130a is an oncomir targeting *CRMP4* and could be developed as a potential prognostic factor and a novel therapeutic target in gastric cancer.

Keywords: gastric cancer, microRNA-130a, miR-130a, *CRMP4*

Introduction

Gastric cancer is a poorly understood, aggressive disease, and has a substantial impact on health worldwide.[1] Although the incidence and mortality rate of gastric cancer have been steadily declined in recent decades due to advances in medical therapies, it is estimated that there are still more than 950,000 new cases of gastric cancer diagnosed per year, with more than 720,000 deaths, making it the fourth most common type of cancer globally and the third leading cause of cancer-related mortality, following lung and liver cancer.[2]

The predominant risk factors influencing the onset and progression of gastric cancer include dietary habits (such as consumption of salt and nitrite-containing foods), smoking, obesity, *Helicobacter pylori* infection, pernicious anemia, and chronic atrophic gastritis.[3,4] Generally, patients suffering from gastric cancer have

Correspondence: Zhiqiang Shen
Department of Pharmacy, Kunming Medical University, 1168#, West Chunrong Road, Kunming, People's Republic of China
Tel +86 182 0873 1160
Email km201704@126.com

submit your manuscript | www.dovepress.com
Dovepress
http://dx.doi.org/10.2147/OTT.S139443

no pathognomonic symptoms in the early stages of disease, where multimodal treatment strategies (eg, complete surgical resection, chemotherapy, and radiotherapy) could cure a proportion of patients and reduce the rate of systemic metastasis.[1,5] Hence, disease is frequently detected at a very advanced stage, resulting in poor clinical outcomes, unfeasibility of advanced treatments, and ultimately mortality.[5,6] The identification of more specific and sensitive novel markers for gastric cancer is urgently required to enable establishment of early screening/identification strategies. In-depth investigation of the molecular basis, pathogenesis, and biological features of gastric cancer occurrence and development is of utmost importance for improved selection of effective new agents for targeted treatment. Currently, it is assumed that the multistep process of gastric cancer pathogenesis may originate from a sequential accumulation of various genetic and epigenetic alterations in oncogenes and tumor-suppressor genes, DNA methylation, microRNAs (miRNAs), and long noncoding RNAs (lncRNAs).[7,8]

miRNAs, a class of small, endogenous, single-stranded, noncoding RNA molecules (18–22 nucleotides in length), can regulate gene expression posttranscriptionally by translational inhibition and messenger RNA (mRNA) destabilization, based on sequence complementarity.[9] At least one-third of human mRNAs are regulated by miRNAs, which have important roles in a wide variety of fundamental biological processes, including cell fate determination, hematopoietic lineage differentiation, organ development, immune responses, proliferation, apoptosis, and signal transduction.[10] Thus, it is not surprising that abnormal miRNA expression profiles have been identified in many human diseases, including diabetes, cardiovascular syndromes, nervous system disorders, autoimmune diseases, and cancers.[11] In the context of gastric cancer, numerous reports indicate that aberrant expression of miRNAs contributes to carcinogenesis by altering the expression of oncogenes and tumor suppressors, affecting cell proliferation, apoptosis, motility, and invasion; moreover, changes in these miRNAs are also closely associated with tumor type, tumor stage, and patient survival.[12,13] Therefore, miRNAs have been investigated and developed as potential diagnostic and prognostic biomarkers, or ideal therapeutic targets, at different stages of gastric cancer development in recent years.[14] For example, miR-21 acts as a key oncomir (oncogenic miRNAs upregulated in cancer cells to enhance cell proliferation, inhibit apoptosis, and induce cell invasion and migration) in gastric cancer by targeting the tumor-suppressor genes, phosphatase and tensin homolog (*PTEN*) and programmed cell death 4 (*PDCD4*).[15,16] In contrast, miR-148a is considered a tumor suppressor in gastric cancer, which can suppress tumor cell invasion by down-regulation of Rho-associated coiled-coil-containing protein kinase 1 (*ROCK1*).[17]

Collapsin response mediator proteins (CRMPs) were originally identified in the nervous system and are involved in neuronal development. There are five homologous cytosolic CRMPs, CRMP1–5,[18] and they are also implicated in cell proliferation, apoptosis, differentiation, and invasion during progression and metastasis of several malignant tumors.[19] For example, CRMP1 promotes lung cancer cell invasiveness[20] and CRMP2 is involved in breast cancer progression.[21] *CRMP4* expression levels are intimately related to lymph node metastasis, tumor node metastasis (TNM) stage, tumor differentiation, and poor prognosis in gastric cancer patients and may have clinical implications including an association with reduced survival rates.[22] To explore the mechanisms underlying the involvement of *CRMP4* in gastric cancer, we predicted upstream regulatory miRNAs using software (TargetScan, miRanda, and miRDB) and literature searches and found that miR-130a potentially regulates *CRMP4*. Accumulating evidence supports a role for miR-130a as an oncomir influencing gastric cancer tumorigenesis.[23,24] Herein, in the current study, we aimed to verify the interaction between miR-130a and *CRMP4* and determine the precise roles of these molecules in gastric cancer. Our results suggest novel strategies for the diagnosis and therapy of gastric cancer.

Materials and methods

Cell lines and culture

The human gastric epithelial cell line, GES-1, and five human gastric cancer cell lines, BGC823, GC9811, HGC-27, MGC-803, and NCI-N87, purchased from American Type Culture Collection (ATCC, Manassas, VA, USA), were maintained in Dulbecco's Modified Eagle's Medium (DMEM; Corning Incorporated, Corning, NY, USA) containing 10% fetal bovine serum (FBS; Thermo Fisher Scientific, Waltham, MA, USA), 100 U/mL penicillin, and 100 µg/mL streptomycin, and incubated at 37°C in a humidified 95% air and 5% CO_2 atmosphere. Cells were subcultured using 0.25% trypsin/EDTA solution (Thermo Fisher Scientific) every 2–3 days. The 293T cells, also obtained from ATCC, were cultured in Roswell Park Memorial Institute (RPMI) 1640 medium (Corning Incorporated) supplemented with 10% FBS and 1% (v/v) penicillin–streptomycin solution at 37°C in a humidified incubator with 95% O_2 and 5% CO_2.

Plasmids and transfection

miR-130a mimics, miR-130a inhibitor, negative control (NC) plasmid, NC inhibitor, *CRMP4* overexpression plasmid, and lentivirus-mediated short hairpin RNA (shRNA) for silencing *CRMP4* were designed and synthesized by Sangon Biotech (Shanghai, China). Cells were seeded into six-well plates at a density of 2×10^5 cells/well and, the following day when the cells were approximately 80% confluent, transfected with the indicated plasmids using FuGENE® HD Transfection Reagent (Promega Corporation, Fitchburg, WI, USA) according to the manufacturer's instructions. After transfection (48 h), cells were collected for the studies as described in the following sections.

RNA extraction and quantitative reverse transcription polymerase chain reaction (qRT-PCR)

Each of the abovementioned six strains of human gastric cells (1×10^6) was harvested and total RNA isolated using Trizol Reagent (Tiangen, Bejing, People's Republic of China), according to the manufacturer's guidelines. The quality and concentration of total RNA were determined using a BioPhotometer, and the integrity of total RNA was assessed by agarose–formaldehyde gel electrophoresis. First-strand complementary DNA (cDNA) was reverse transcribed from total RNA using an Moloney Murine Leukemia Virus (M-MLV) Reverse Transcriptase Kit (Promega Corporation) following the manufacturer's protocols. Then, the cDNA was subjected to PCR amplification using an ABI Prism® 7500 Sequence Detection System (Thermo Fisher Scientific) and an SYBR Green qPCR SuperMix Kit (Thermo Fisher Scientific) with the following conditions: 2 min of pre-denaturation at 95°C, followed by 40 cycles of 15 s of denaturation at 95°C, 32 s of annealing at 60°C (with data collection at the end of the 60°C step of each cycle). A melting curve was then generated. Primer sequences for the amplification of *CRMP4*, *18S rRNA* (as an internal control for *CRMP4*), miR-130a, and U6 snRNA (as an internal control for miR-130a) are listed in Table 1. The fold change in *CRMP4* and miR-130a expression levels was calculated using the $2^{-\Delta\Delta Ct}$ method, and all reactions, including no template controls, were performed in triplicate.

Western blot (WB)

Cell lysates were prepared in 100–200 µL radioimmunoprecipitation assay lysis buffer (Beyotime, Nantong, People's Republic of China), supplemented with 1% protease and phosphatase inhibitor cocktail (Beyotime), for 20 min on ice and protein content quantified using a bicinchoninic acid

Table 1 Sequences of primers used for qRT-PCR assays

Gene or miRNA	Primer sequences
CRMP4	Forward primer: 5′-CATTCACTCCACCTGATCTC-3′ Reverse primer: 5′-CCCTCCTTCTTCTGCTCC-3′
18S rRNA	Forward primer: 5′-CCTGGATACCGCAGCTAGGA-3′ Reverse primer: 5′-GCGGCGCAATACGAATGCCCC-3′
miR-130a	RT primer: 5′-GTCGTATCCAGTGCAGGGTCCGAGG TGCACTGGATACGACATGCCCT-3′ Forward primer: 5′-TTGCGATTCTGTTTTGTGCT-3′ Reverse primer: 5′-GTGGGGTCCTCAGTGGG-3′
U6 snRNA	RT primer: 5′-CTCAACTGGTGTCGTGGAGTCGGCA ATTCAGTTGAGAAAAATA[illegible]C-3′ Forward primer: 5′-CT[illegible]CTTCG[illegible]AGCACA-3′ Reverse primer: 5′-A[illegible]CGCTTCACG[illegible]TTTGCGT-3′

Abbreviation: qRT-PCR, quantitative reverse transcription polymerase chain reaction.

Protein Assay Kit (Beyotime). Denatured proteins (30 µg) were separated on 8%–15% discontinuous sodium dodecyl sulfate (SDS)-polyacrylamide gels by electrophoresis and then electrophoretically transferred to polyvinylidene difluoride (PVDF) membranes. After blocking with 5% skimmed milk in phosphate-buffered saline (PBS) with 0.1% Tween-20 for 2 h at room temperature, PVDF membranes were incubated overnight at 4°C with *CRMP4* (Abcam, Cambridge, UK) or GAPDH (Boster, Wuhan, People's Republic of China) primary antibodies at dilutions of 1:1,000 and 1:500, respectively. For immunodetection, membranes were incubated with secondary antibodies (SouthernBiotech, Guangzhou, People's Republic of China) at dilutions of 1:4,000 (anti-mouse) and 1:5,000 (anti-rabbit) for 1 h at room temperature. Finally, blots were developed using an Immobilon Western Chemilum HPR Substrate Kit (EMD Millipore, Billerica, MA, USA) and exposed to X-ray film (Kodak, Tokyo, Japan).

Plasmid construction and luciferase reporter assay

psiCHECK-2 vector was purchased from Sangon Biotech and used to construct the recombinant vectors, WT-*CRMP4*-3′UTR, which contained a putative *CRMP4* 3′ untranslated region (UTR) target region for miR-130a, and Mutant-*CRMP4*-3′UTR in which the target sequence was mutated. The 293T cells were plated in 24-well plates at a density of 1.0×10^5/well, cultured to achieve approximately 80% confluence, and co-transfected with WT-*CRMP4*-3′UTR plasmid, Mutant-*CRMP4*-3′UTR plasmid, psiCHECK-2 vector (ie, blank group), miR-130a mimics, miR-130a inhibitor, NC plasmid, or NC inhibitor, using Lipofectamine 2000 (Promega Corporation) according to the manufacturer's recommendations. After an additional

48 h of incubation with these plasmids, luciferase and renilla signals were assayed using the Dual-Luciferase® Reporter Assay System (Promega Corporation). All experimental transfection procedures were repeated at least three times.

Flow cytometry

Flow cytometry was used to determine apoptosis and cell cycle regulation of BGC823 cells transfected with NC, *CRMP4* overexpression, miR-130a mimics, and *CRMP4* + miR-130a plasmids. For the apoptosis assay, 48 h post transfection, cells were detached by trypsinization, collected by centrifugation at 15,000 rpm for 5 min, and incubated with 250 µL Annexin V binding buffer and 10 µL freshly prepared Annexin V–propidium iodide (PI) mixed reagent (Beyotime) per sample, followed by thorough mixing in the dark at 37°C for 15 min. Thereafter, samples were analyzed within 30 min on a FACScan flow cytometer.

For cell cycle assays, cells were treated as described earlier, then collected, fixed with chilled 70% ethanol, and stored overnight at −20°C. The following day, after washing twice with ice-cold PBS, cells were resuspended in 400 µL staining solution containing 0.5 µg/mL RNase A and 50 µg/mL PI for 30 min at 37°C in the dark and analyzed using flow cytometry.

Cell proliferation assay

Cell proliferation was estimated using 3-(4,5-dimethylthiazol-2-yl)-2,5-diphenyltetrazolium bromide (MTT) reagent (Promega Corporation), according to the manufacturer's protocols. The proliferation of BGC823 cells transfected with the abovementioned plasmids in 96-well plates was monitored every day for 3 days. At the indicated time points after transfection, 20 µL MTT working solution was added into the wells, followed by incubation at 37°C for 4 h. Subsequently, the culture medium was removed and the formazan crystals formed by MTT treatment solubilized in 150 µL dimethylsulfoxide (DMSO) solution for 20 min. Absorbance at 570 nm was then measured using a microplate reader (Bio-Rad Laboratories Inc., Hercules, CA, USA), with a reference wavelength of 630 nm. Each treatment group was composed of three separate wells.

Colony formation assay

After 48 h, transfected BGC823 cells were mixed with 0.3% soft agar in DMEM containing 10% FBS, plated in six-well culture dishes at a density of 300 cells/well, and coated with 0.6% solidified agar in DMEM containing 10% FBS, in triplicate. The culture medium was replaced with fresh DMEM every 3 days and after 14 days cultured at 37°C, the resulting colonies were fixed with methanol at −20°C for 5 min, and then stained with 0.005% crystal violet (Sigma-Aldrich Co., St Louis, MO, USA). The number of clearly visible colonies (diameter >50 µm) in three random microscopic fields was counted, and the images were captured under a microscope (Leica Microsystems, Wetzlar, Germany) and analyzed using ImageJ software.

In vitro cell invasion, cell migration, and cell adhesion assay

Transfected BGC823 cells were grown in serum-free medium until they were 90%–100% confluent in 24-well Transwell chambers with 8 µm pore size membranes (BD Biosciences, San Jose, CA, USA) and a thin layer of matrigel basement membrane matrix (BD Biosciences). Simultaneously, 600 µL of complete culture medium containing 10% FBS was added to the lower compartment and placed in 5% CO_2 atmosphere saturated with H_2O at 37°C. Following 24 h of incubation, noninvasive cells were gently scraped off using a cotton swab and invasive cells on the bottom surface of the insert were fixed with 4% paraformaldehyde for 10 min and then stained with 0.01% crystal violet in 20% ethanol for 15 min. Finally, cells in at least three randomly selected microscopic fields under a light microscope were photographed and counted. To further assess cell migration, assays were conducted as mentioned earlier except that the transfected BGC823 cells were cultivated on top of uncoated (Matrigel-free) filters. In addition, cell adhesion assays were carried out using matrigel-precoated 96-well culture plates (BD Biosciences). Following the indicated transfections, BGC823 cells were seeded in matrigel-precoated 96-well culture plates and incubated for 1 h at 37°C. Then, non-adherent cells were removed using a cotton swab, 50 µL of MTT solution (5 mg/mL) was added to each well, and plates were maintained at 37°C in a humidified incubator for an additional 4 h. Next, 200 µL of DMSO was added to each well, followed by the measurement of optical density (OD) values at 570 nm on a microplate reader.

Nude mice tumor xenograft model

Five-week-old athymic BALB/c nude mice weighing 18–22 g were obtained from the Experimental Animal Center of Yan'an Hospital Affiliated to Kunming Medical University, bred in a standard specific pathogen-free environment with an alternating 12 h light/dark cycle at 25°C±2°C, and provided with free access to aseptic food and water. All the animal care and experimental procedures were approved by the Animal Care and Use Committee of Yan'an Hospital Affiliated to Kunming Medical University and compliant with the Yan'an Hospital Affiliated to Kunming Medical

University Committee Guidelines on the Use of Live Animals in Research, which is according to the National Institutes of Health (NIH) Guide for the Care and Use of Laboratory Animals (NIH Publications no 80-23), revised 2010.

To compare the tumorigenicity of BGC823 cells transfected with NC plasmid, *CRMP4*-shRNA, miR-130a mimic, and miR-130a mimic + *CRMP4*-shRNA, we injected these cells subcutaneously into the dorsal flanks of nude mice randomly divided into the three groups with five mice per group. Tumor volume was measured 7 days after injection using calipers and calculated by the modified ellipsoidal formula: tumor volume (mm^3) = (length [mm]) × (width [mm])^2/2. All mice were sacrificed under anesthesia, and the dissected tumors were weighed immediately, 23 days after transplantation. Tumor samples from all groups were used for the detection of miR-130a and *CRMP4* expression levels by qRT-PCR, WB, and immunohistochemical staining.

Immunohistochemical staining

Tumor tissue sections were deparaffinized in xylene, dehydrated with graded ethanol, blocked with 0.3% hydrogen peroxide in methanol for 15 min at room temperature, and boiled in 0.01 M sodium citrate buffer (pH 6.0) in a microwave oven for 10 min for antigen epitope retrieval. After cooling for 20 min at room temperature and washing with distilled water, slides were incubated with primary rabbit polyclonal antibodies against *CRMP4* at 37°C for 2 h, followed by washing three times with PBS. Immunostaining was detected using the EnVision™ + System (Boster, Wuhan, China) according to the manufacturer's guidelines. Finally, slides were washed with PBS, counterstained with Mayer's hematoxylin, dehydrated through an alcohol gradient, and sealed with cover slips. Images were captured under an optical microscope.

Statistical analysis

All statistical calculations were performed using SPSS 18.0 software (SPSS Inc., Chicago, IL, USA). Values are expressed as mean ± standard deviation (SD) from three independent experiments, and values of $P<0.05$ or 0.01 were considered statistically significant. Two-tailed Student's *t*-tests and one-way analysis of variance (ANOVA) were applied to assess the statistical significance of differences between two, or among more than two, groups, respectively.

Results

CRMP4 expression in six human gastric cell lines

We compared the mRNA and protein levels of *CRMP4* between the human gastric epithelial cell line, GES-1, and five human gastric cancer cell lines, BGC823, GC9811, HGC-27, MGC-803, and NCI-N87, by qRT-PCR and WB. *CRMP4* mRNA expression was significantly decreased in human gastric cancer cell lines compared with GES-1 (Figure 1A). Furthermore, WB demonstrated that, compared with GES-1 cells, *CRMP4* protein expression was much lower in human gastric cancer cell lines, particularly BGC823, GC9811, and HGC-27 (Figure 1B). In addition, miR-130a expression in the five human gastric cancer cell lines was higher than that in GES-1 cells (Figure 1C). These data suggest that *CRMP4* expression is reduced, while that of miR-130a is elevated, in human gastric cancer cell lines.

CRMP4 is a novel target gene of miR-130a

Bioinformatics analysis predicted that miR-130a was a potential direct regulator of *CRMP4* and accumulating evidence supports a role for miR-130a in the occurrence and development of gastric cancer. To further investigate whether miR-130a can mediate the decay of *CRMP4* mRNA via binding to its 3′UTR, dual luciferase reporter assays were performed in 293T cells. As illustrated in Figure 2A, plasmid containing putative miR-130a-binding sites in *CRMP4* and corresponding mutant sites were generated. Next, these constructs were co-transfected into 293T cells with psiCHECK-2 empty vector, miR-130a mimics, miR-130a inhibitor, NC plasmid, or NC inhibitor. The results indicated that miR-130a dramatically reduced the luciferase activity of the WT-*CRMP4* construct, while the luciferase activity of the WT-*CRMP4* construct was clearly increased following transfection with miR-130a inhibitor, NC plasmid, and NC inhibitor. There were no changes in luciferase activity from the Mutant-*CRMP4* construct following co-transfection with these plasmids (Figure 2B). Moreover, *CRMP4* mRNA and protein expressions levels were significantly decreased in BGC823 cells pre-transfected with miR-130a mimic, whereas those in BGC823 cells pre-transfected with miR-130a inhibitor were markedly increased (Figure 2C and D). These results demonstrate that miR-130a can directly regulate *CRMP4* by targeting its 3′UTR.

miR-130a inhibited BGC823 apoptosis, induced cell cycle arrest in G1 phase, and accelerated proliferation by targeting *CRMP4*

To investigate the effects of miR-130a and *CRMP4* on BGC823 apoptosis, apoptotic cells were labeled and detected

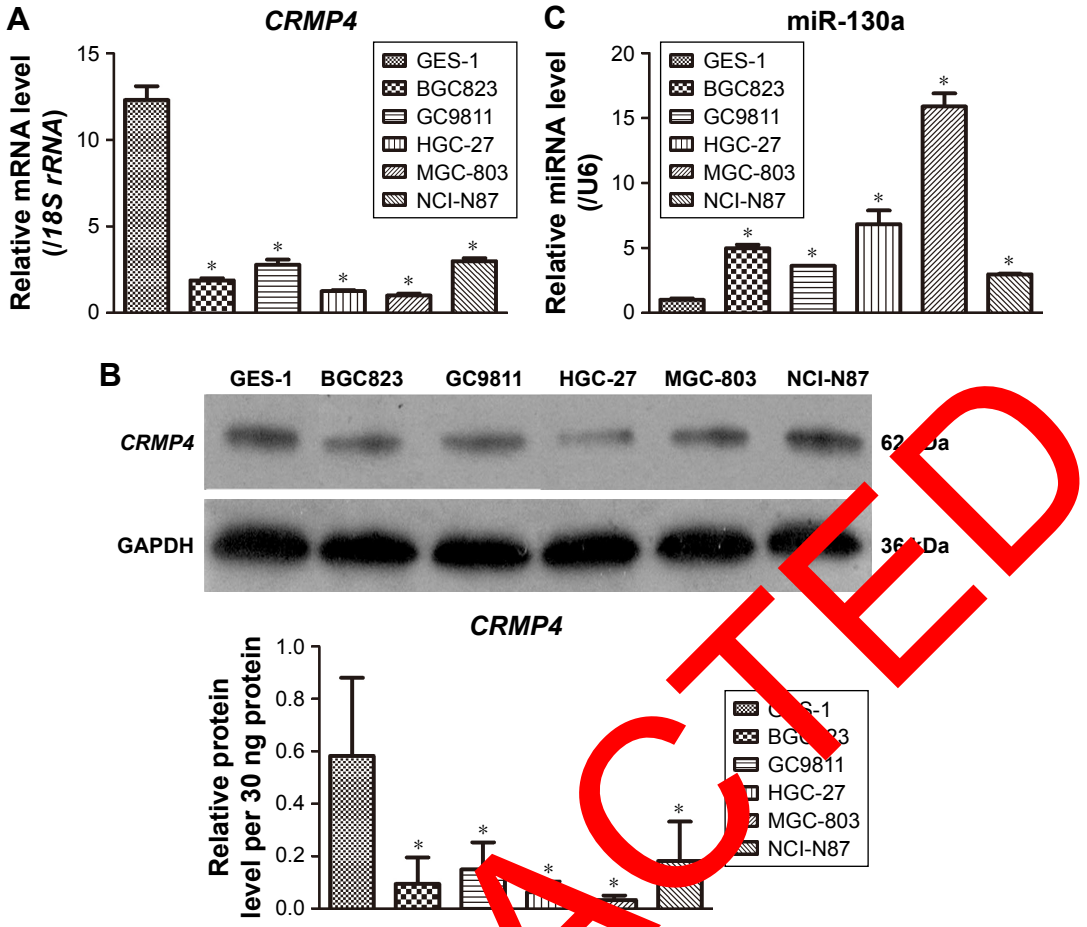

Figure 1 *CRMP4* expression patterns determined by qRT-PCR and W
Notes: (**A**) Bar graph of *CRMP4* mRNA expression determine by qRT-PCR in six human gastric cell lines, normalized to *18S rRNA* expression (n=3). (**B**) Six human gastric cell lines were subjected to WB analysis of *CRMP4* and GAPDH (loading control). (**C**) miR-130a expression was examined by qRT-PCR in six human gastric cell lines (normalized to U6 snRNA expression; n=3). *$P<0.05$.
Abbreviations: qRT-PCR, quantitative reverse transcription polymerase chain reaction; WB, Western blot.

using Annexin V/PI staining and flow cytometry. As depicted in Figure 3A, there were no clear differences in early apoptosis (Annexin V^+/PI^-) among the groups; however, in comparison with the NC and *CRMP4* + miR-130a group, late apoptosis (Annexin V^+/PI^+) was notably upregulated in the *CRMP4* group and correspondingly downregulated in the miR-130a group.

We next examined alterations of the cell cycle in BGC823 cells subjected to different treatments. Compared with those in the NC and *CRMP4* + miR-130a groups, the *CRMP4* overexpression group showed a decrease in the proportion of cells in the G1 phase and an increase of those in the S phase, whereas there was a substantial increase in BGC823 cells in the G1 phase following treatment with miR-130a mimics (Figure 3B).

Finally, we assessed the effect of miR-130a and *CRMP4* on cell proliferation using MTT assays (Figure 3C). Increased *CRMP4* expression led to significant inhibition of cell proliferation. Conversely, treatment with miR-130a remarkably induced cell proliferation. No changes were observed in cell proliferation in the NC and *CRMP4* + miR-130a groups (Figure 3A). Overall, these results indicate the involvement of miR-130a in mediating apoptosis, G1 cell cycle arrest, and proliferation, probably through targeting of *CRMP4*.

CRMP4 reversed the effect of miR-130a-mediated promotion of gastric cancer colony formation, cell invasion, cell migration, and cell adhesion

To elucidate whether miR-130a can regulate BGC823 cell growth through *CRMP4*, soft agar colony formation assays were carried out. As shown in Figure 4A, cells transfected with *CRMP4* overexpression plasmid showed reduced colony formation compared with those transfected with the

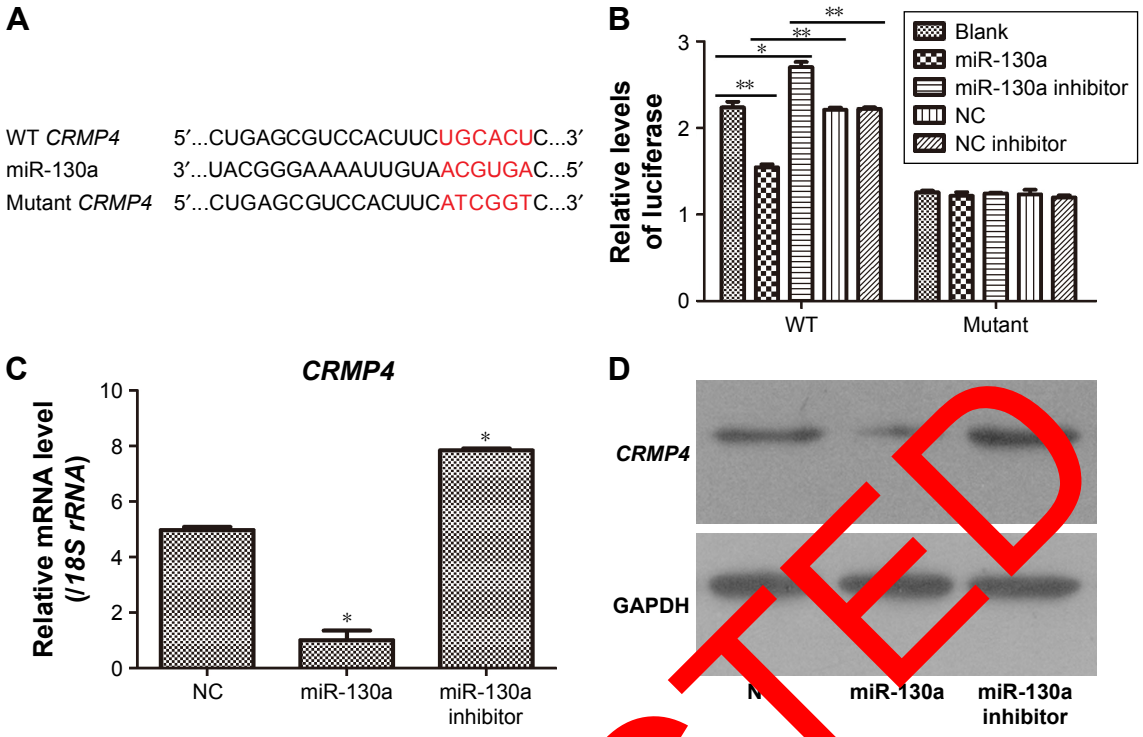

Figure 2 miR-130a targeted the 3′UTR of *CRMP4*.

Notes: (**A**) Schematic of the putative miR-130a binding sites in the *CRMP4*-3′UTR predicted using miRanda and the mutant miR-130a sites in the *CRMP4*-3′UTR designed by Sangon Biotech. (**B**) Dual-luciferase reporter assays were performed in 293T cells. **P*<0.05, ***P*<0.01. (**C**) The level of *CRMP4* gene expression was analyzed by qRT-PCR. **P*<0.05 (**D**) *CRMP4* protein level was determined by WB.

Abbreviations: NC, negative control; qRT-PCR, quantitative reverse transcription polymerase chain reaction; WB, Western blot; WT, Wild type.

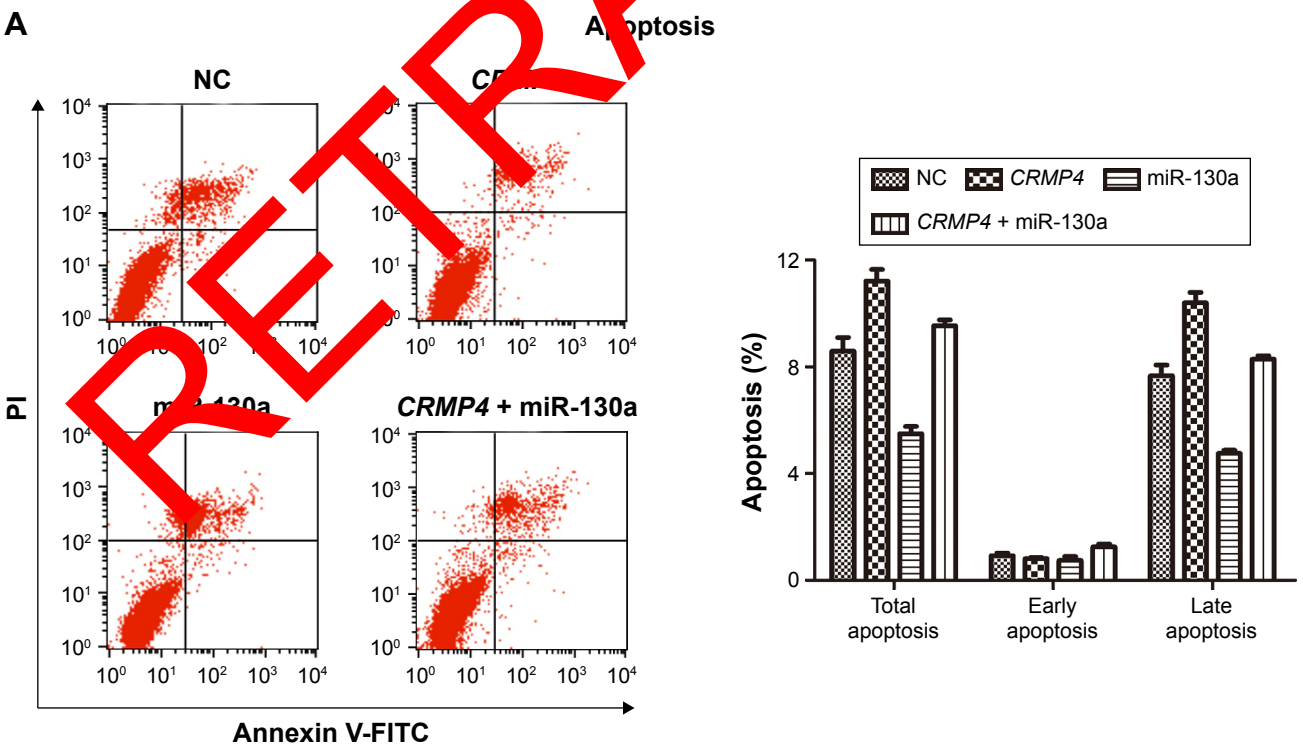

Figure 3 (*Continued*)

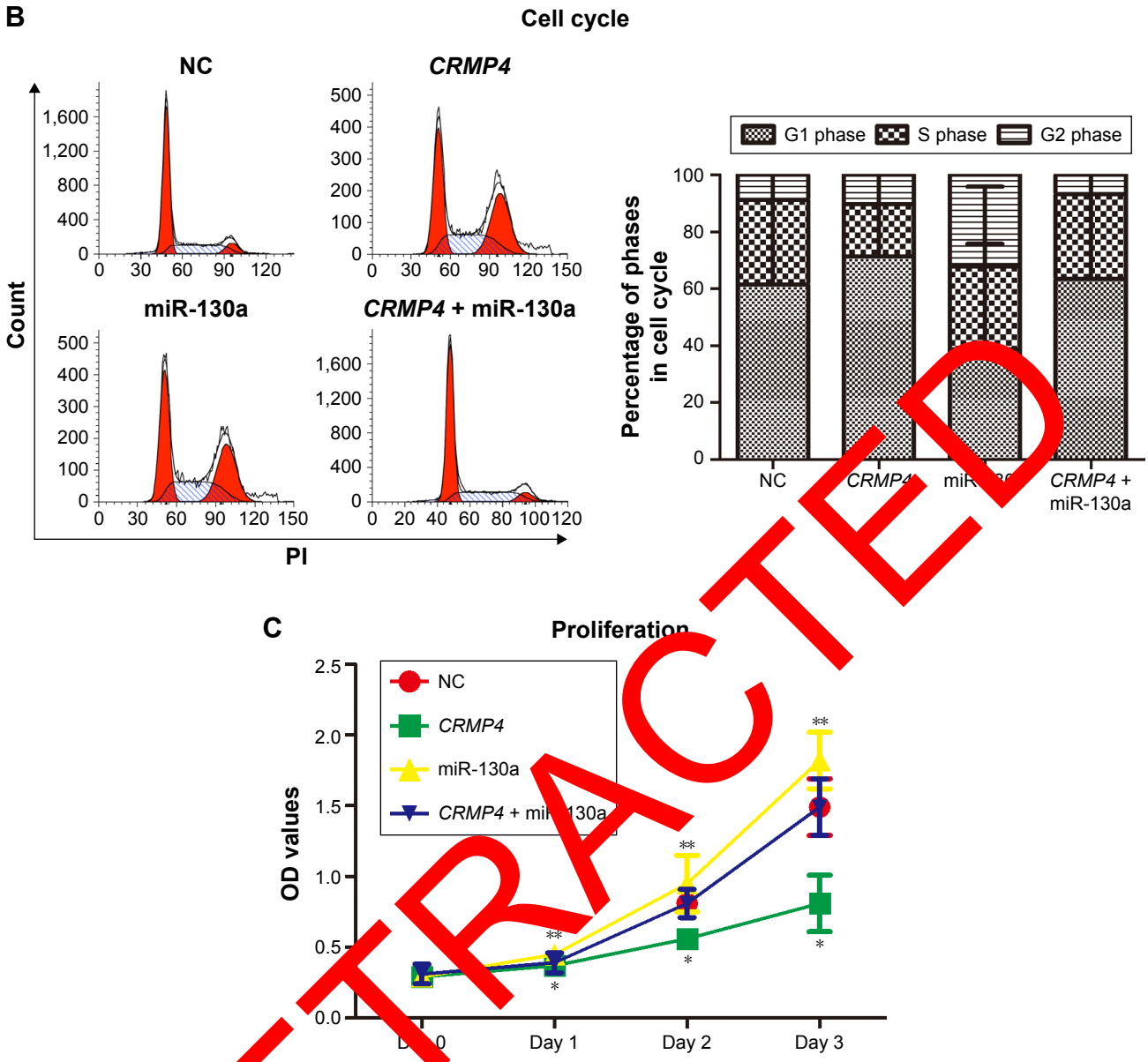

Figure 3 Evaluation of apoptosis, cell cycle, and proliferation in BGC823 cells.
Notes: (**A**) miR-130a inhibited apoptotic death of BGC823 cells induced by *CRMP4*, as determined using flow cytometric analysis. (**B**) miR-130a arrested BGC823 cells in the G1 phase of the cell cycle through effects on *CRMP4*, as determined by flow cytometry. (**C**) miR-130a suppressed cell proliferation in BGC823 cells via *CRMP4* as detected by MTT assay. $^{*}P<0.05$, $^{**}P<0.01$.
Abbreviations: FITC, fluorescein isothiocyanate; NC, negative control; PI, propidium iodide.

vector only control, while cells transfected with miR-130a mimics exhibited increased colony formation. The relative colony formation ratio of the *CRMP4* + miR-130a group was similar to that of the NC group in soft agar colony formation assays.

Consistent with our observations in the colony formation assays, we measured cell invasion and migration utilizing Transwell assays in vitro and found that augmented *CRMP4* expression greatly decreased the migratory and invasive behaviors of BGC823 cells, whereas elevated miR-130a expression reduced these characteristics in BGC823 cells transfected with *CRMP4* overexpression plasmid (Figure 4B and C).

To evaluate the cell adhesion capacity of BGC823 cells after treatment with different plasmids, we performed MTT assays by the detection of OD values at 570 nm (Figure 4D). The results demonstrated that the adhesive ability of BGC823 cells transfected with miR-130 mimics was stronger than those transfected with *CRMP4* overexpression plasmid. In addition, the OD values of the NC group were markedly higher than those of the *CRMP4* group. There was no significant difference between NC and *CRMP4* + miR-130a groups.

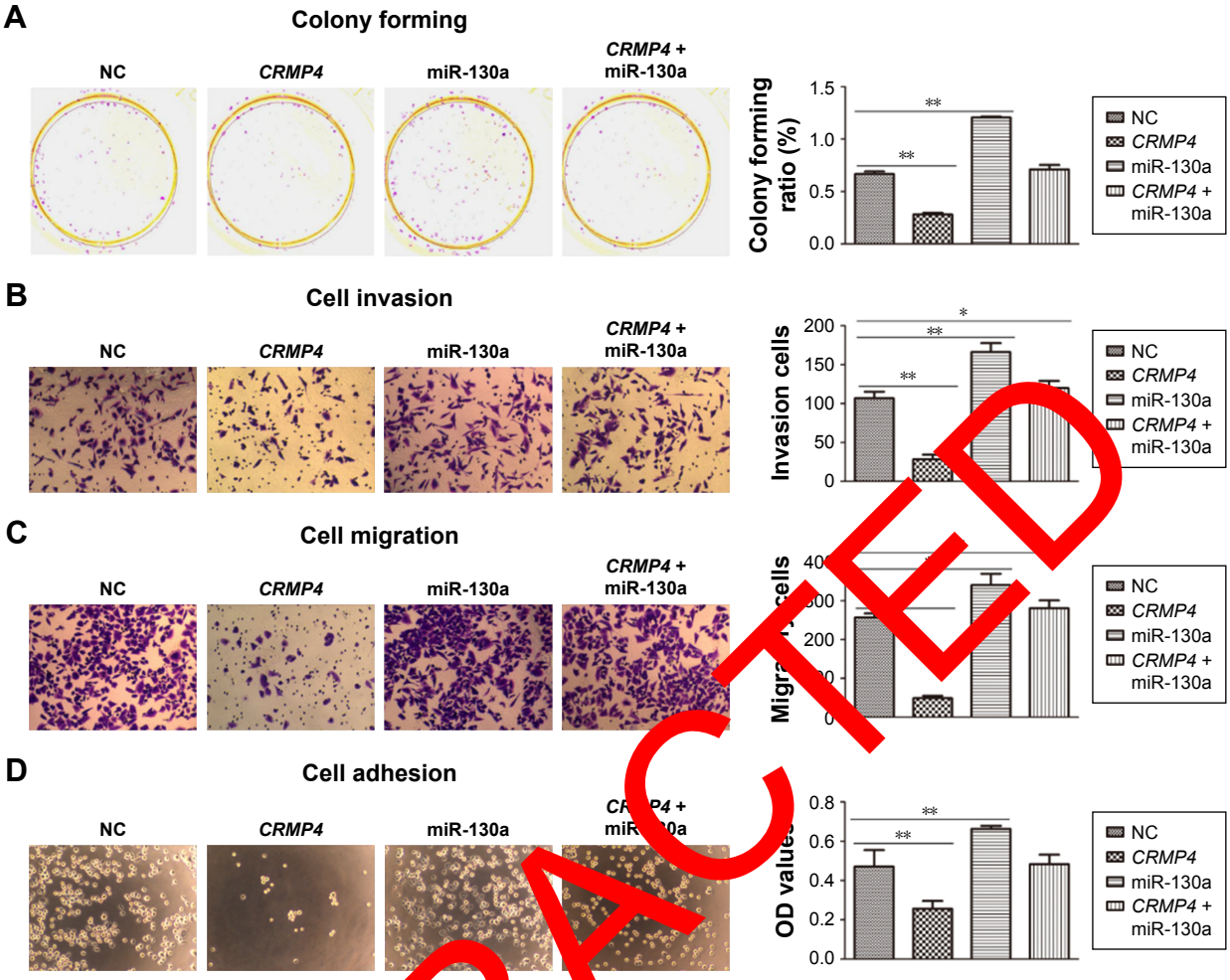

Figure 4 Effects of miR-130a and *CRMP4* on BGC823 [illegible] colony fo[illegible]ation, invas[illegible], migration, and adhesion in vitro.
Notes: Representative images of each group are prese[illegible]d in th[illegible] statistical histograms are provided in the right panel. *$P<0.05$ and **$P<0.01$. (**A**) Colony formation of BGC823 cells transfected with dif[illegible]ent plas[illegible]magnification 100×). (**B**) Cell invasiveness was evaluated using Transwell invasion assays. (**C**) BGC823 cell migration after transfection with plasmids ov[illegible]xpressing *CR*[illegible]or miR-130a. (**D**) Adhesion of BGC823 cells transfected with different plasmids in vitro.
Abbreviation: NC, negative control.

Collectively, these fi[illegible]ngs indicate that mi[illegible]-130a facilitates colony formation, invasi[illegible], migration, and adhesion of BGC823 cells, where[illegible]upregula[illegible]n of *CRMP4* abolished these effe[illegible]s of m[illegible]-130a.

CRMP4 suppressed tumor growth in nude mouse models

Based on the results of the abovementioned studies, we hypothesized that *CRMP4* knockdown in BGC823 cells may have antitumor effects in vivo. To address this hypothesis, we established an in vivo pretreated xenograft nude mouse model. First, to verify the transfection efficiency of miR-130a mimic and/or *CRMP4*-shRNA in mice tissue samples from all groups, the expression levels of miR-130a and *CRMP4* were examined. Our results revealed that miR-130a expression was clearly upregulated in the miR-130a and miR-130a + *CRMP4*-shRNA groups (Figure 5A), while *CRMP4* expression was notably downregulated in the *CRMP4*-shRNA, miR-130a, and miR-130a + *CRMP4*-shRNA groups at both the mRNA and protein levels (Figure 5B–D). Moreover, in these five groups (Figure 6A) of nude mice, tumors formed on the 12th day after subcutaneous injection and their growth was observed for 23 days. Compared to the BGC823 and NC groups, depletion of *CRMP4* resulted in clear retardation of tumor growth in vivo; after 23 days, BGC823 cells transfected with *CRMP4*-shRNA, miR-130a mimic, and miR-130a mimic + *CRMP4*-shRNA produced smaller tumors, compared with BGC823 cells alone and transfected with NC plasmid (Figure 6B).

Discussion

Gastric cancer remains one of the most common malignant tumors worldwide and is a serious threat to human health.[25]

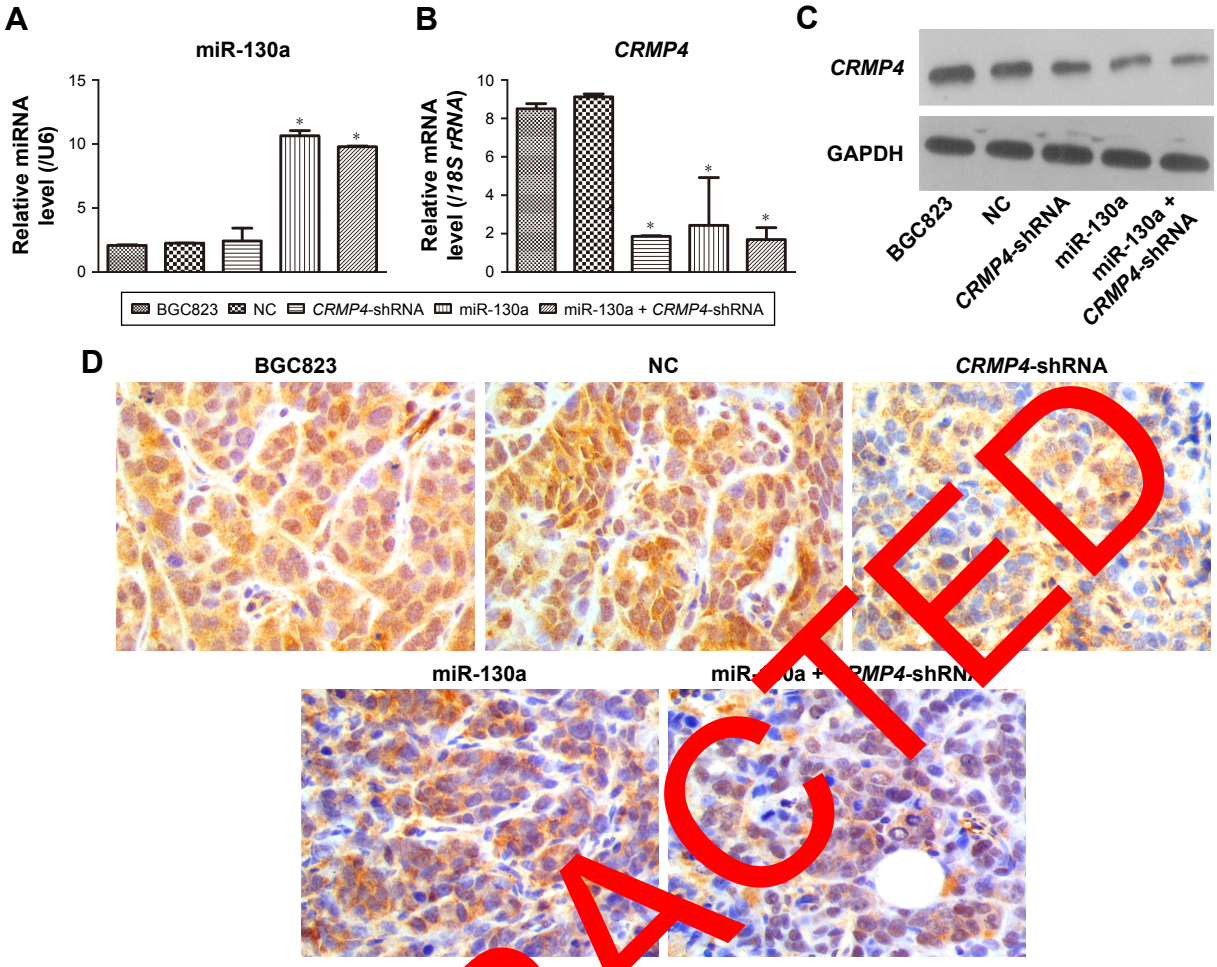

Figure 5 Expression levels of miR-130a and *CRMP4* in the tumor xenograft nude mouse model.
Notes: (**A**) miR-130a expression determined by qRT-PCR. *$P<0.05$. (**B**) *CRMP4* expression determined by qRT-PCR. *$P<0.05$. (**C**) *CRMP4* expression determined by WB. (**D**) *CRMP4* expression detected by immunohistochemical staining.
Abbreviations: NC, negative control; qRT-PCR, quantitative reverse transcription polymerase chain reaction; WB, Western blot.

Despite remarkable progress in the diagnosis and treatment of gastric cancer in recent decades, the prognosis for patients remains dismal, primarily due to systemic metastasis and postoperative recurrence. Recently, a large body of studies have demonstrated that gastric cancer is a multistage process resulting from the accumulation of genetic and epigenetic alterations, particularly aberrant expression of miRNAs.[27] miRNAs have emerged as critical regulators of gene expression at the posttranscriptional level and are mediators of cancer-related development, progression, metastasis, and processes related to prognosis.[28] Hence, the functions of cancer-related miRNAs have been explored to better understand carcinogenesis and identify cancer biomarkers. Previous studies have demonstrated that miR-130a is implicated as an oncomir contributing to the pathogenesis of many human cancers, including gastric cancer, hepatocellular carcinoma, non-small cell lung cancer, colon cancer, pancreatic cancer, and breast cancer.[29] In addition, *CRMP4* can facilitate gastric tumor growth and metastasis;[30,31] however, the biological roles and molecular mechanisms underlying miR-130a and *CRMP4* involvement in the modulation of the malignant behavior of gastric cancer cells are largely unknown. Interestingly, we predicted an interaction between miR-130a and *CRMP4* using TargetScan, miRanda, and miRDB software, through direct targeting of the 3′UTR region of *CRMP4*. Therefore, in the current study, we investigated the detailed biological roles of miR-130a and *CRMP4* in gastric cancer. First, we examined the gene and protein expression levels of *CRMP4* in different gastric cancer cell lines and discovered that they were significantly downregulated compared with GES-1 cells, which is consistent with previous studies of patient gastric cancer tissues.[22] This result indicates that low *CRMP4* expression levels may have an important function in gastric cancer in vitro, as well as in vivo. Subsequently, a dual-luciferase reporter assay using cells transfected with WT- and Mutant-*CRMP4* 3′UTR recombinant plasmids

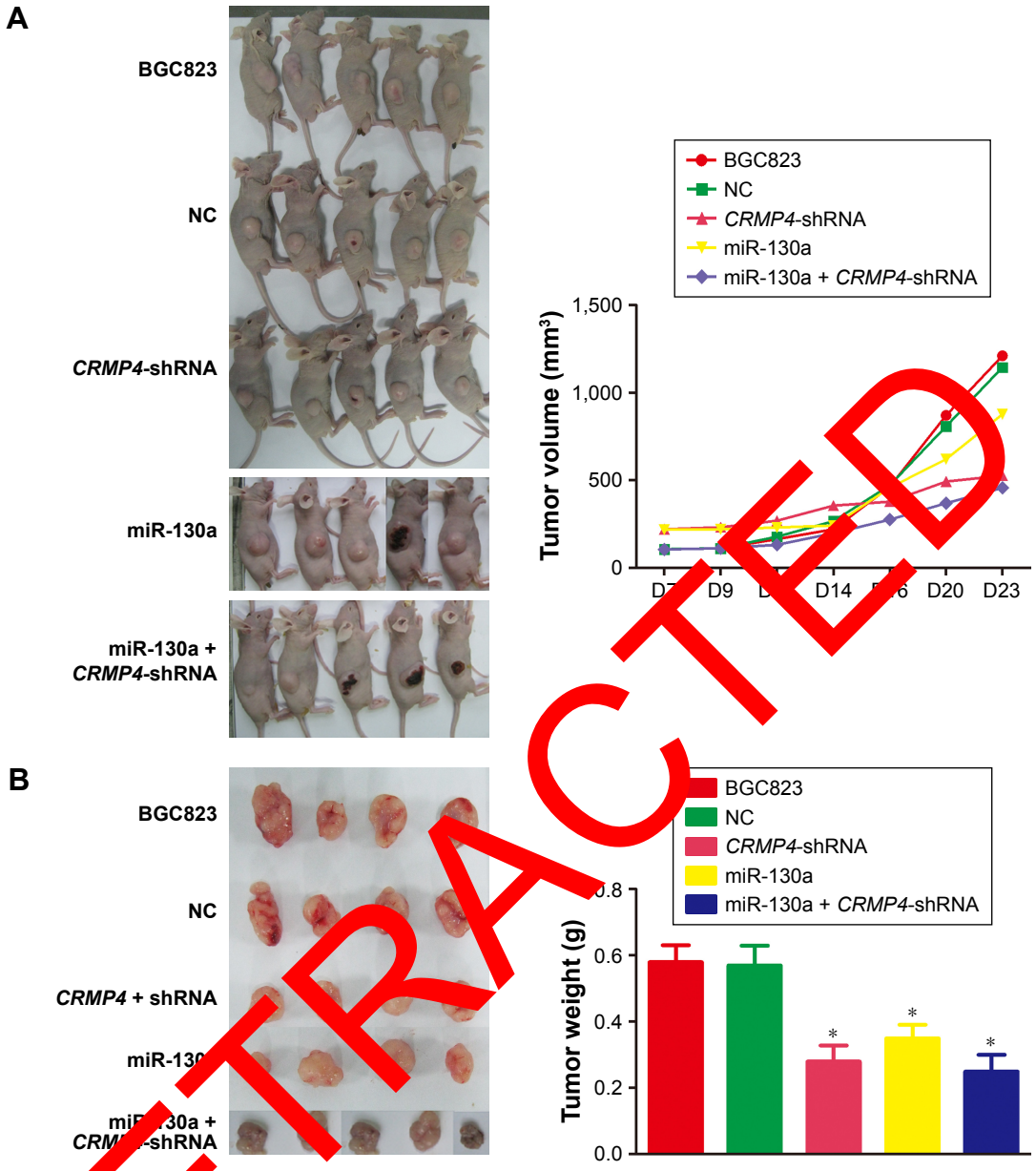

Figure 6 In vivo tumorigenicity of BGC823 cells after different treatments.
Notes: (**A**) Representative images of mice injected with BGC823 cells subjected to different treatments and a growth curve of tumor volume from days 7 to 23 are presented. (**B**) Representative images of tumors completely removed from mice and the weights of tumors from each group are presented. *$P<0.05$.
Abbreviations: D, days; NC, negative control.

revealed that there were remarkable inverse correlations between miR-130a and *CRMP4* expression levels, suggesting that *CRMP4* is a direct target of miR-130a, and implying that miR-130a and *CRMP4* may constitute an intricate and accurate regulatory circuit in the development and progression of gastric cancer.

In this study, to elucidate the biological functions of miR-130a in gastric cancer through targeting of *CRMP4*, experiments were performed to evaluate gastric cancer cell apoptosis, cycle, proliferation, colony formation, migration, invasion, and adhesion. Dysregulation of apoptosis and the cell cycle are intimately associated with tumor growth.[32] A series of studies have revealed that numerous miRNAs are implicated in the regulation of apoptosis and the cell cycle by targeting the apoptosis-related genes, *Bcl-2* and *Bax*, and the cell cycle-related genes, *cyclinA1*, *cyclinB1*, and *cyclinD2*, during the process of gastric cancer pathogenesis.[33–36] Our data demonstrate that the overexpression of *CRMP4* could clearly promote apoptosis and induce cell cycle arrest in BGC823 cells in comparison with miR-130a treatment, indicating that miR-130a may modulate the growth of BGC823 tumor cells via targeting of *CRMP4*. In addition,

cell proliferation and colony formation are major processes implicated in malignant tumor progression.[32,37] Our results demonstrate that miR-130a can markedly accelerate cell proliferation and colony formation of BGC823 cells, which in turn, stimulate the development of tumors. Conversely, *CRMP4* reversed the effects of miR-130a in promoting cell proliferation and colony formation. Upregulation of miR-130a in gastric cancer cells has previously been reported to promote their proliferation.[23] Overall, these findings lead us to conclude that miR-130a can facilitate tumor progression of BGC823 cells through the suppression of *CRMP4*.

The effects of miR-130a and *CRMP4* on cell migration, invasion, and adhesion, which are considered indicative of tumor metastasis events,[38] were also examined in our study. BGC823 cells transfected with miR-130a mimics exhibited greatly increased cell migration, invasion, and adhesion ability; however, BGC823 cells transfected with *CRMP4* lost these characteristics. Nevertheless, miR-130a has previously been reported as enhancing migration and invasion ability in human cervical cancer SiHa cells,[39] and *CRMP4* expression is inversely correlated with lymph node metastasis in pancreatic cancer.[30] These observations provide further confirmation that miR-130a can enhance metastatic qualities of BGC8[illegible] tumor cells by attenuating *CRMP4* expression.

We next established a tumor xenograft mod[illegible] in nude mice to evaluate the function of *CRMP4* in [illegible]stric [illegible]ncer in vivo and discovered that knockout o[illegible] *CRMP*[illegible]ing siRNA markedly inhibited tumor xeno[illegible]raft gr[illegible]h and led to a reduced tumor volume, suppo[illegible]g our in vit[illegible] results. However, in a study of colon [illegible]ancer, [illegible]eatment of colon cancer cells with miR-130a [illegible]nhibitor in a [illegible]mor xenograft model resulted in dela[illegible]d tumo[illegible] formation,[39] consistent with our results regardi[illegible] the [illegible]rgeted interaction between miR-130a and *CRMP4*. He[illegible], these d[illegible]a provide confirmation of the rol[illegible] of miR[illegible]130a as [illegible]comir in gastric cancer through rep[illegible]ssion o[illegible] *CRMP4*.

Conclusion

We report significantly reduced expression of *CRMP4* in gastric cancer cell lines and its direct targeting by miR-130a, closely associated with gastric cancer growth, progression, and metastasis. These results may not only assist in expansion of knowledge of the functions of miR-130a and *CRMP4* during gastric cancer pathogenesis but also provide a potential new biomarker for the early detection of gastric cancer and therapeutic target for the treatment of patients with this disease.

Disclosure

The authors report no conflicts of interest in this work.

References

1. Mihmanli M, Ilhan E, Idiz UO, Alemdar A, Demir U. Recent developments and innovations in gastric cancer. *World J Gastroenterol*. 2016; 22(17):4307–4320.
2. Majeed W, Iftikhar A, Khaliq T, et al. Gastric carcinoma: recent trends in diagnostic biomarkers and molecular targeted therapies. *Asian Pac J Cancer Prev*. 2016;17(7):3053–3060.
3. Cheng XJ, Lin JC, Tu SP. Etiology and prevention of gastric cancer. *Gastrointest Tumors*. 2016;3(1):25–36.
4. Compare D, Rocco A, Nardone G. Risk factors in gastric cancer. *Eur Rev Med Pharmacol Sci*. 2010;14(4):302–308.
5. Berger H, Marques MS, Zietlow R, [illegible]eyer [illegible] Machado JC, Figueiredo C. Gastric cancer patho[illegible]nesis. *Helico[illegible]cter*. 2016; 21(suppl 1):34–38.
6. den Hoed CM, Kuipers EJ. G[illegible]ic can[illegible] how can [illegible] reduce the incidence of this disease? *C[illegible] Gastroenterol Rep*. 20[illegible];18(7):34.
7. Patel TN, Roy S, Ravi R[illegible]stric can[illegible] and re[illegible]pigenetic alterations. *Ecancermedicalsc[illegible]ce*. 201[illegible]1:714.
8. Fu DG. Epigenetic [illegible]eration[illegible]stric cance[illegible]Review). *Mol Med Rep*. 2015;12(3):3223[illegible]230.
9. Treiber T, Tr[illegible] J, Meister G. [illegible]ion of microRNA biogenesis and functi[illegible]. *Throm[illegible]Haemost*. 2012;107(4):605–610.
10. Krol J, Loedige I, F[illegible]owicz W. The widespread regulation of mi[illegible]RNA biogenesis, [illegible]tion and decay. *Nat Rev Genet*. 2010; [illegible]9):597–610.
11. [illegible]ul P, Chakrab[illegible]y A, Sarkar D, et al. Interplay between miRNAs and [illegible]man diseases: [illegible]eview. *J Cell Physiol*. Epub 2017 Feb 9.
12. W[illegible]WK, Lee C[illegible], Cho CH, et al. MicroRNA dysregulation in gastric c[illegible]ew player enters the game. *Oncogene*. 2010;29(43): [illegible]5761–5771.
13. [illegible]H, Kimura M, Takeyama H. Role of microRNAs in gastric cancer. *World J Gastroenterol*. 2014;20(19):5694–5699.
14. Wang F, Sun GP, Zou YF, Hao JQ, Zhong F, Ren WJ. MicroRNAs as promising biomarkers for gastric cancer. *Cancer Biomark*. 2012;11(6): 259–267.
15. Sekar D, Krishnan R, Thirugnanasambantham K, Rajasekaran B, Islam VI, Sekar P. Significance of microRNA 21 in gastric cancer. *Clin Res Hepatol Gastroenterol*. 2016;40(5):538–545.
16. Li L, Zhou L, Li Y, Lin S, Tomuleasa C. MicroRNA-21 stimulates gastric cancer growth and invasion by inhibiting the tumor suppressor effects of programmed cell death protein 4 and phosphatase and tensin homolog. *J BUON*. 2014;19(1):228–236.
17. Zheng B, Liang L, Wang C, et al. MicroRNA-148a suppresses tumor cell invasion and metastasis by downregulating ROCK1 in gastric cancer. *Clin Cancer Res*. 2011;17(24):7574–7583.
18. Yamashita N, Goshima Y. Collapsin response mediator proteins regulate neuronal development and plasticity by switching their phosphorylation status. *Mol Neurobiol*. 2012;45(2):234–246.
19. Tan F, Thiele CJ, Li Z. Collapsin response mediator proteins: potential diagnostic and prognostic biomarkers in cancers (Review). *Oncol Lett*. 2014;7(5):1333–1340.
20. Wang WL, Hong TM, Chang YL, Wu CT, Pan SH, Yang PC. Phosphorylation of LCRMP-1 by GSK3beta promotes filopodia formation, migration and invasion abilities in lung cancer cells. *PLoS One*. 2012; 7(2):e31689.
21. Shimada K, Ishikawa T, Nakamura F, et al. Collapsin response mediator protein 2 is involved in regulating breast cancer progression. *Breast Cancer*. 2014;21(6):715–723.
22. Chen S, Zhang X, Peng J, et al. VEGF promotes gastric cancer development by upregulating CRMP4. *Oncotarget*. 2016;7(13):17074–17086.
23. Lee SH, Jung YD, Choi YS, Lee YM. Targeting of RUNX3 by miR-130a and miR-495 cooperatively increases cell proliferation and tumor angiogenesis in gastric cancer cells. *Oncotarget*. 2015;6(32):33269–33278.

24. Jiang H, Yu WW, Wang LL, Peng Y. miR-130a acts as a potential diagnostic biomarker and promotes gastric cancer migration, invasion and proliferation by targeting RUNX3. *Oncol Rep*. 2015;34(3):1153–1161.
25. Goral V. Etiopathogenesis of gastric cancer. *Asian Pac J Cancer Prev*. 2016;17(6):2745–2750.
26. Liu L, Cao L, Gong B, Yu J. Novel biomarkers for the identification and targeted therapy of gastric cancer. *Expert Rev Gastroenterol Hepatol*. 2015;9(9):1217–1226.
27. Katona BW, Rustgi AK. Gastric cancer genomics: advances and future directions. *Cell Mol Gastroenterol Hepatol*. 2017;3(2):211–217.
28. Li M, Li J, Ding X, He M, Cheng SY. microRNA and cancer. *AAPS J*. 2010;12(3):309–317.
29. Liu L, Nie J, Chen L, et al. The oncogenic role of microRNA-130a/301a/454 in human colorectal cancer via targeting Smad4 expression. *PLoS One*. 2013;8(2):e55532.
30. Gao X, Pang J, Li LY, et al. Expression profiling identifies new function of collapsin response mediator protein 4 as a metastasis-suppressor in prostate cancer. *Oncogene*. 2010;29(32):4555–4566.
31. Guo H, Xia B. Collapsin response mediator protein 4 isoforms (CRMP4a and CRMP4b) have opposite effects on cell proliferation, migration, and invasion in gastric cancer. *BMC Cancer*. 2016;16:565.
32. Evan GI, Vousden KH. Proliferation, cell cycle and apoptosis in cancer. *Nature*. 2001;411(6835):342–348.
33. Zhu FQ, Zeng L, Tang N, et al. MicroRNA-155 downregulation promotes cell cycle arrest and apoptosis in diffuse large B-cell lymphoma. *Oncol Res*. 2016;24(6):415–427.
34. Zhang BC, Zhou ZJ, Sun L. pol-miR-731, a teleost miRNA upregulated by megalocytivirus, negatively regulates virus-induced type I interferon response, apoptosis, and cell cycle arrest. *Sci Rep*. 2016;6:28354.
35. Li P, Xie XB, Chen Q, et al. MiRNA-15a mediates cell cycle arrest and potentiates apoptosis in breast cancer cells by targeting synuclein-gamma. *Asian Pac J Cancer Prev*. 2014;15(16):6949–6954.
36. He JF, Luo YM, Wan XH, Jiang D. Biogenesis of MiRNA-195 and its role in biogenesis, the cell cycle, and apoptosis. *J Biochem Mol Toxicol*. 2011;25(6):404–408.
37. Wang Y, Zhang P, Liu Z, et al. CUL4A overexpression enhances lung tumor growth and sensitizes lung cancer cells to erlotinib via transcriptional regulation of EGFR. *Mol Cancer*. 2014;13:252.
38. Geng HT, Cao RJ, Cheng L, Liu CY. Overexpression of hepatocyte cell adhesion molecule (hepaCAM) inhibits the proliferation, migration and invasion in colorectal cancer cells. *Oncol Res*. Epub 2016 Dec 15.
39. He L, Wang HY, Zhang L, et al. Prognostic significance of low DICER expression regulated by miR-130a in cervical cancer. *Cell Death Dis*. 2014;5:e1205.